Structure Characteristics in Industrially Centrifugally Cast 25Cr20Ni Stainless Steel Tubes Solidified under Different Electromagnetic Field Intensity

X.Q. Wu, Y.S. Yang, J.S. Zhang, G.L. Jia, and Z.Q. Hu

(Submitted 11 September 1998; in revised form 8 February 1999)

The influences of different electromagnetic field intensities on the solidification structures of industrially centrifugally cast 25Cr20Ni stainless steel tubes have been investigated in detail. The results reveal that the electromagnetic field exerted during the centrifugal solidification causes a marked variation in the structures of the cast tubes. With an increase of the electromagnetic field intensity, the area fraction of the equiaxed structures in transverse sections of the cast tubes increases, and the macrostructures are gradually refined. The distribution of the eutectic carbides changes from the dendrite boundaries to the grain boundaries. However, an excessive electromagnetic field intensity gives rise to many intergranular cast defects formed along the inner walls of the centrifugally cast tubes. The effects of fluid flow induced by the electromagnetic field on the solidification process of the centrifugally cast tubes are the primary reason for the previously mentioned structure variations.

Keywords austenitic stainless steel, centrifugal cast, electromagnetic field, solidification process

1. Introduction

A 25Cr20Ni austenitic stainless steel has been widely used as a tube material for steam reforming operations in the petrochemical industry since the 1960s. Due to higher carbon content (approximately 0.4 wt%), the steel is commonly used in the form of centrifugally cast tubes. Its solidification structures usually consist of austenite matrix supersaturated with carbon and eutectic carbide (M_7C_3) distributed along the grain and dendrite boundaries. During service at high temperatures, a substantial quantity of nonhomogeneous secondary carbide particles ($M_{23}C_6$) are precipitated in the tubes. The eutectic carbides formed initially, and the secondary carbides precipitated during service are the main strengthening factors of the 25Cr20Ni stainless steel tubes in long term service.

With rapid development of the petrochemical industry, the steam reforming operation tends to develop toward a higher temperature and a shorter period gradually. It is unavoidable to give rise to an increasing demand on the mechanical properties of the reforming tubes, especially the elevated temperature creep properties. During the last three decades, many researchers have devoted themselves to the study of optimizing the solidification structures and improving the mechanical properties of 25Cr20Ni stainless steel tubes (Ref 1-7). The main method is to raise the nickel content (from 20 to 35 or 45 wt%) in tube materials and to introduce some alloying elements such as silicon, niobium, titanium, zirconium, tungsten, and molybdenum. Raising the nickel content can stabilize the austenite and decrease the solution of carbon in austenitic matrix (Ref 8), thus promoting more strengthening phases precipitated at the grain and dendrite boundaries, which can retard dislocation movement and improve the elevated temperature strength (Ref 9). The higher silicon content in tube materials, up to 2 wt%, is effective to improve the surface coking and carburizing resistance of the reforming tubes (Ref 10-11). The addition of niobium, titanium, zirconium, tungsten, and molybdenum to Fe-Cr-Ni alloys can improve the types and distribution of eutectic carbides and precipitated secondary carbides and increase the resistance to creep deformation of tube materials. As a result, a new generation of heat-resistant tube materials such as HP50-WNb, KHR35CW, and PG28485 were developed and successfully applied in fabricating the petrochemical tubes.

However, more complex chemical compositions require more complicated melting operation and a higher fabrication cost; moreover, the increase of nickel content in tube materials strongly promotes surface coking and carburizing (Ref 12). For avoiding these shortcomings and further enhancing the mechanical properties of cast reforming tubes, a cast process connecting the electromagnetic force field and the centrifugal force field has been developed and applied in industry production in recent years (Ref 13-15). In this article, the authors report on the structure characteristics of industrially centrifugally cast 25Cr20Ni stainless steel tubes solidified under different electromagnetic field intensity and discuss the effects of the electromagnetic field on the centrifugal solidification process of the cast tubes.

2. Experimental Procedure

Figure 1 shows a schematic of the equipment diagram of industrially electromagnetic centrifugal cast tubes. The rotating cams are driven by an electric motor with a rotating velocity that can be adjusted conveniently. The electromagnetic

X.Q. Wu, Y.S. Yang, J.S. Zhang, G.L. Jia, and **Z.Q. Hu,** Department of Superalloy and Special Casting, Institute of Metal Research, Chinese Academy of Sciences, 72 Wenhua Road, Shenyang 110015, P.R. China.

field intensity can be controlled successively by adjusting the exciting magnetic current in coils. The cast mold with a length of 300 cm and an inner diameter of 19 cm consists of nonmagnetic cast steel.

Table 1 lists the compositions of the stainless steel used in the experiments. Three industrial tubes, A1, A2, and A3, are cast by using the electromagnetic centrifugal equipment. The order of increasing exciting current is: A1, A2, A3. All the metallographic specimens are cut from the middle region of industrially electromagnetic centrifugal cast tubes (i.e., 150 cm from the cool end of the cast tubes) and prepared in terms of the standard metallographic method. The mean sizes of grains are determined by employing a lineal analyzing technique.

3. Experimental Results

Figure 2 shows the macrostructures in transverse sections of the industrially electromagnetic centrifugal cast tubes. It is clear that increasing the exciting current during the centrifugal solidification strongly promotes development of the equiaxed structures along the radial direction of the cast tubes. Moreover, both the columnar structures and the equiaxed structures are markedly refined by the introduction of an electromagnetic field. In addition, distinguished with the conventional centrifugal cast tubes whose columnar grains grow along the radial direction of tubes, most of columnar grains in the electromagnetic centrifugal cast tubes develop slanted along the radial direction. Table 2 lists the area fraction of the columnar structures and the equiaxed structures as well as the grain sizes of the cast tubes.

Figure 3 shows the dendrite morphologies of the electromagnetic centrifugal cast tubes. To identify the dendrite clearly, all specimens were aged for 1 h. Because the secondary carbides were precipitated along the grain and dendrite boundaries, it is easy to observe the dendrite morphologies by using a light microscope. From Fig. 3, it can be seen that with an increase of the exciting current during the centrifugal solidification, the growth of the dendrites previously along the radial direction of the cast tubes is disturbed gradually. The first dendrite arms become narrow, and the fronts of the dendrites begin bending, branching, and breaking.

Figure 4 illustrates the microstructures of the electromagnetic centrifugal cast tubes. Clearly the electromagnetic field exerted during the centrifugal solidification promotes the distribution of the eutectic carbides changes from the dendrite boundaries to the grain boundaries. Moreover, with an increase of the exciting current, the blocky eutectic carbides initially distributed along the dendrite boundaries disappear gradually. Instead, a host of skeletonlike carbides are precipitated along the grain boundaries.

Table 1 Compositions of 25Cr20Ni steel used in experiments

	Composition, wt%								
Steel	**Cr**	**Ni**	**C**	**Si**	**Mn**	**Mo**	**S**	**P**	**Fe**
25Cr20Ni	25.48	21.39	0.41	1.16	0.73	0.01	0.005	0.018	bal

Table 2 Area fraction of macrostructures and grain sizes of cast tubes

Tube code	Area fraction of columnar structure, %	Area fraction of equiaxed structure, %	Mean width of columnar grain, μm	Mean length of columnar grain, mm	Mean size of equiaxed grain, μm
A1	95	0	463	8.1	…
A2	52.9	41.2	373	4.6	273
A3	32.3	58.1	288	3.4	62

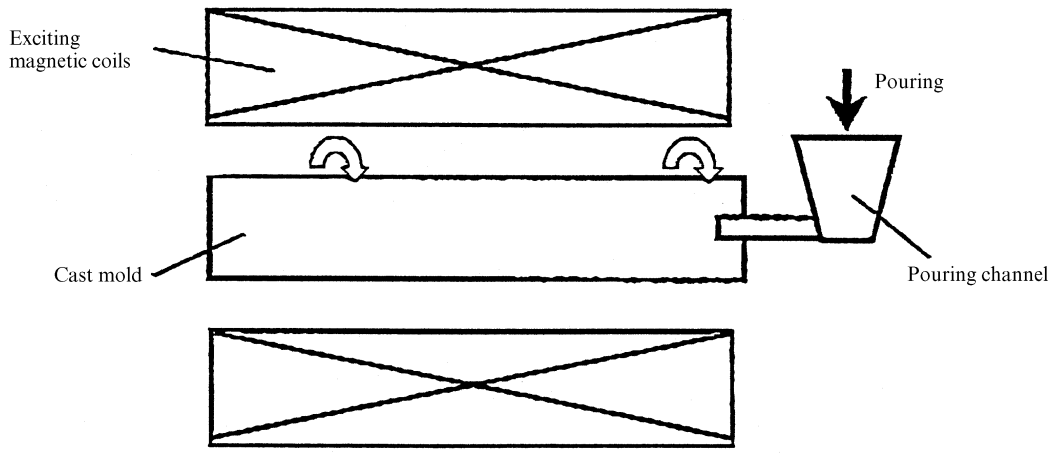

Fig. 1 Schematic diagram of equipment of industrially electromagnetic centrifugal cast tubes

It is worthy to note that there are many intergranular cast defects distributed in the inner wall of tube A3, as shown by Fig. 5(a). This reveals that an excessive electromagnetic field intensity is not beneficial to the microstructures of the centrifugally cast tubes. Figure 5(b) shows the morphology of the secondary carbides precipitated near the defects after 1 h aging. Clearly, the secondary carbides are seriously precipitated in the grains surrounded by the intergranular defects. The farther the grains near the defects, the less the precipitated carbides, and the smaller the size of the secondary carbides.

4. Discussion

During the centrifugal solidification, the liquid steel rotates with the cast mold at a higher speed, *V*. When a stationary magnetic field, *B*, is introduced, the relative motion is built between the liquid steel and the magnetic field. Then according to the Maxwell equations and Ohm's law, an induction current, *I*, is produced through the liquid steel, and the interaction between the induction current and the magnetic field results in the Lorenz force, F_e, (Ref 16):

$$F_e = I \times B = \sigma(V \times B) \times B \quad \text{(Eq 1)}$$

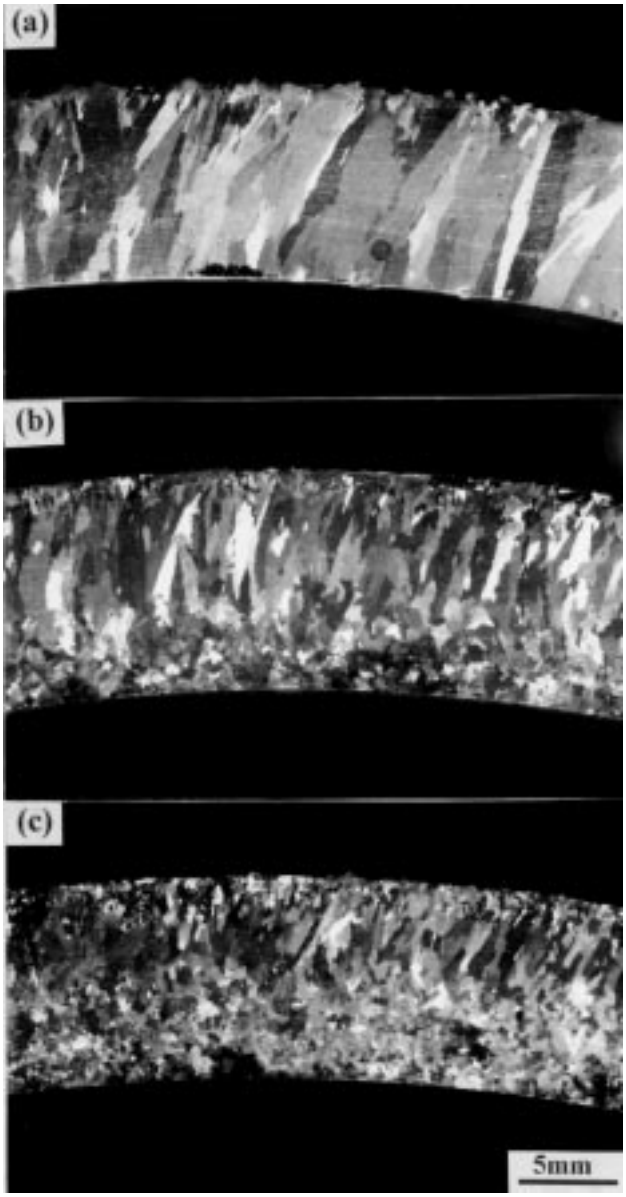

Fig. 2 Macrostructures of industrially electromagnetic centrifugal cast tubes. (a) Tube A1. (b) Tube A2. (c) Tube A3

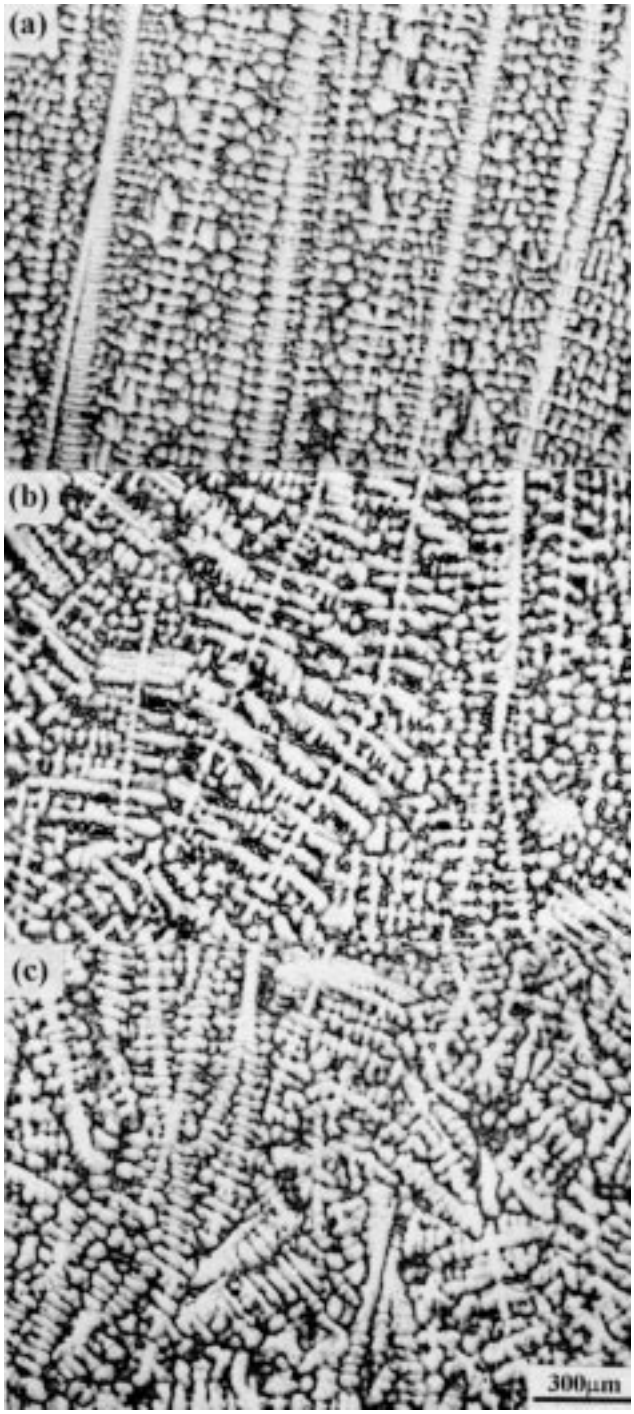

Fig. 3 Dendrite morphologies of industrially electromagnetic centrifugal cast tubes. (a) Tube A1. (b) Tube A2. (c) Tube A3

where σ is the electric conductivity of the liquid steel. Driven by F_e, a fluid flow contrary to the direction of rotation is induced in the liquid steel in front of the solid/liquid interface. Clearly the higher the exerted exciting magnetic current, the stronger the fluid flow ahead of the solid/liquid interface.

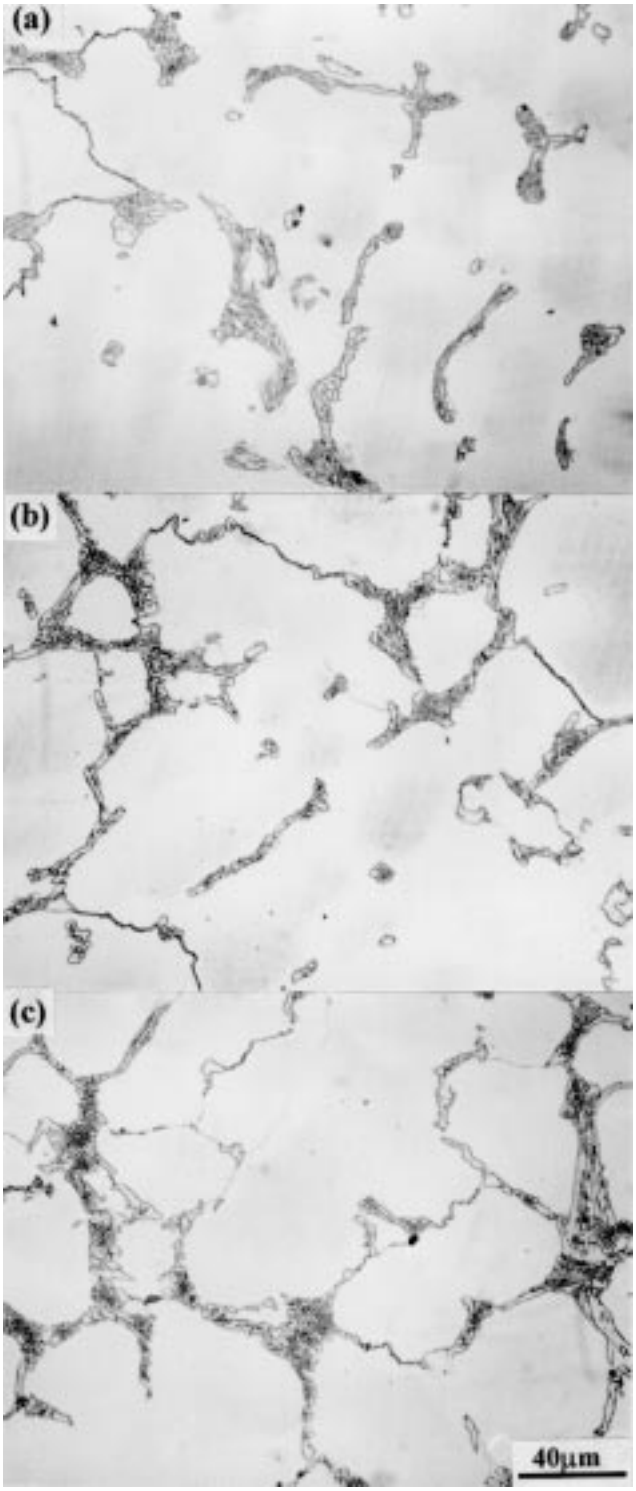

Fig. 4 Microstructures of industrially electromagnetic centrifugal cast tubes. (a) Tube A1. (b) Tube A2. (c) Tube A3

The effects of the electromagnetic field on the solidification structures of the centrifugally cast tubes are closely related to the fluid flow stated previously. In general, the growth direction of the columnar grains is contrary to direction of the thermal dissipation. During the centrifugal solidification, the direction of the thermal transportation is parallel to normal direction of the outer surface of the cast tubes. So the columnar grains grow along the radial direction of the tubes. Because the fluid flow induced by F_e is nearly normal to the growth direction of grains and can easily remove the aggregated solutes on the side of the grains facing the flow, the growth of upstream direction of the columnar grains is accelerated. This results in the inclined columnar grains formed in the outer wall of the cast tubes. The fluid flow also accelerates the thermal transfer from the bulk liquid to the solidification front and homogenizes the temperature distribution in the residual liquid (Ref 17). As a possible result, the liquid temperature near the solid/liquid interface and the temperature gradient ahead of the solid/liquid

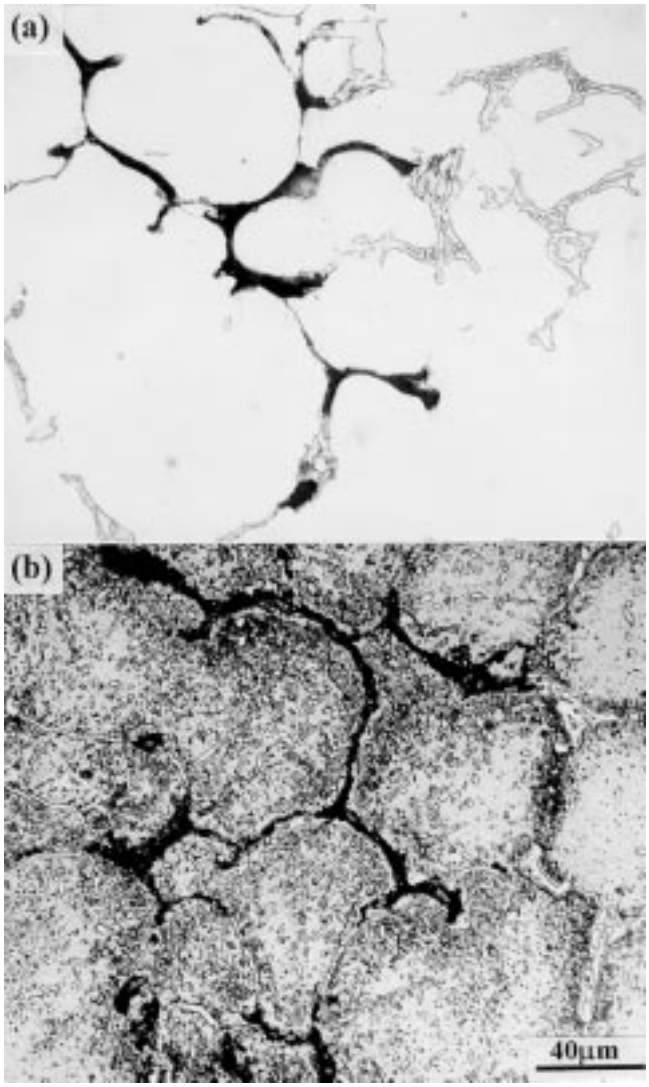

Fig. 5 Intergranular cast defects in inner wall of industrially electromagnetic centrifugal cast tube A3. (a) Intergranular defects. (b) Secondary carbides near the defects after aging 1 h

interface increases. Such an increase of the temperature gradient should promote the development of the columnar grains along the radial direction of the cast tubes. However, as stated previously in the experimental results, with an increase of the exciting magnetic current, the area fraction of the columnar structures in the transverse section of the cast tubes decreases gradually, which seems to contradict the previous argument.

In fact, with an increase of the temperature near the solid/liquid interface, the superheated liquid can penetrate the permeable mushy zone and cause a localized remelting of dendrites (Ref 18-19). Moreover, the fluid flow induced by F_e frequently erodes the solid/liquid interface and can also give rise to a mechanical damage to the solidification front. Consequently, the dendrite fronts are bent, branched, and even broken as illustrated by Fig. 3, and many fragments are easily produced. Thereafter, these fragments resulting from the remelting or the mechanical damage can be removed into the residual liquid by the fluid flow. Because the fluid flow promotes the thermal transfer from the bulk liquid to the solidification front and in turn leads to a decrease of the temperature in the residual liquid, these fragments may easily survive and become the nuclei of the equiaxed grains. Moreover, the simultaneous nucleation may occur in the relatively cool residual liquid. Therefore, with enhancing of the fluid flow, the growth of the columnar grains is retarded, and a large number of the equiaxed grains are developed in the inner wall of the centrifugally cast tubes (Fig. 1). In addition, because the fluid flow strongly promotes the nucleation of grains even during the early stage of solidification, both the columnar grains and the equiaxed grains are refined gradually with an increase of the exciting magnetic current.

The solidification process of 25Cr20Ni stainless steel includes $L \rightarrow \gamma$ and $L \rightarrow \gamma + M_7C_3$ (Ref 20). In the case of a small exciting magnetic current (tube A1), the fluid flow induced by the electromagnetic stirring is weak, the primary growth type of γ grains is columnar, and the solute atoms rejected from solid phase at the solid/liquid interface during the solidification are aggregated at the dendrite boundaries. So after complete solidification, many eutectic structures are distributed along the dendrite boundaries. With an increase of the exciting magnetic current (tube A2 and A3), the stronger fluid flow promotes the columnar-equiaxed transition and accelerates the mass transfer process in the residual liquid, and thus decreases the solute aggregation at the dendrite boundaries. During the later stage of the solidification, the residual liquid mainly exists in the grain boundary zones and thereafter is turned into the intergranular eutectic structures.

However, excessive electromagnetic field intensity will seriously decrease the radial pressure inside the liquid steel during the centrifugal solidification (Ref 21). Therefore, the tightness of the liquid steel will be decreased, and the feeding capacity of the residual liquid to the solidified zone will be weakened. Moreover, the dropping of radial pressure is not beneficial to the exhaust of gas dissolved in the liquid steel. During the later stage of the centrifugal solidification, the shrinkage in final solidification zones in the inner wall of the cast tube cannot be compensated, so many cast defects appear along the grain boundaries in tube A3. The grains surrounded by the defects are the final solidification zones, and the oversaturation degree of the solute in these zones is more serious than that in the normal solidification zones far from the defects. Thus during aging, the secondary carbides are more easily precipitated and coarsened within or near the defect zones as shown by Fig. 5(b).

5. Conclusions

The following conclusions can be drawn:

- The electromagnetic field exerted during solidification of the centrifugally cast tubes causes a marked variation in the structures of the cast tubes. With an increase of the electromagnetic field intensity, the columnar grains grow slanting along the radial direction of the cast tubes, the area fraction of the equiaxed structures in transverse section of the cast tubes increases, and the macrostructures become refined gradually. Moreover, the distribution of the eutectic carbides changes from the dendrite boundaries to the grain boundaries. The primary reason for these structure variations is attributed to influences of the fluid flow induced by the electromagnetic field on the solidification process of the centrifugally cast tubes.
- An excessive electromagnetic field intensity exerted during the centrifugal solidification causes a decrease of the radial pressure inside the liquid steel and thus results in many intergranular cast defects formed in the inner wall of the cast tubes.

Acknowledgments

This study was supported by the Sinopec Technology Company and the Science and Technology Foundation of Liaoning of China.

References

1. L.T. Shinoda, M.B. Zaghloul, Y. Kondo, and R. Tanaka, The Effect of Single and Combined Additions of Ti and Nb on the Structure and Strength of the Centrifugally Cast HK40 Steel, *Trans. ISIJ*, Vol 18, 1978, p 139-148
2. H. Wen-Tai and R.W.K. Honeycombe, Structure of Centrifugally Cast Austenitic Stainless Steels: Part 1 HK40 As Cast and after Creep between 750 and 1000 °C: Part 2. Effects of Nb, Ti, and Zr, *Mater. Sci. Technol.*, Vol 1 (No. 5), 1985, p 385-397
3. G.D. Barbabela, L.H. Almeida, T.L. Silveira, and I. May, Phase Characterization in Two Centrifugally Cast HK Stainless Steel Tubes, *Mater. Char.*, Vol 26 (No. 1), 1991, p 1-7
4. G.D.A. Soares, L.H. Almeida, T.L. Silveira, and I. May, Niobium Additions in HP Heat-Resistant Cast Stainless Steels, *Mater. Char.*, Vol 29 (No. 4), 1992, p 387-396
5. C.W. Thomas, M. Borshevsky, and A.N. Marshall, Assessment of Thermal History of Niobium Modified HP50 Reformer Tubes by Microstructural Methods, *Mater. Sci. Technol.*, Vol 8 (No. 10), 1992, p 855-861
6. R.A.P. Ibanez, G.D.A. Soares, L.H. Almeida, and I. May, Effects of Si Content on the Microstructure of Modified-HP Austenitic Steels, *Mater. Char.*, Vol 30 (No. 4), 1993, p 243-249
7. C.W. Thomas, K.J. Stevens, and M.J. Ryan, Microstructure and Properties of Alloy HP50-Nb: Comparison of As Cast and Service Exposed Materials, *Mater. Sci. Technol.*, Vol 12 (No. 5), 1996, p 469-475
8. J. Liu, Z. Wang, Z. Pan, and B. Sun, Effects of Carbon, Nickel, and Molybdenum on the High Temperature Strength of Fe-Cr-Ni Alloys, *Mater. Trans. JIM*, Vol 37 (No. 2), 1996, p 138-141

9. E.A.A.G. Ribeiro, R. Papaleo, and J.R.C. Guimaraes, Microstructure and Creep Behavior of a Niobium Alloyed Cast Heat-Resistant 26% Cr Steel, *Metall. Mater. Trans.*, Vol 17A, 1986, p 691-696
10. L.H. Wolfe, Laboratory Investigation of High Temperature Alloy Corrosion and Failures, *Mater. Perform.*, (No. 4), 1978, p 38-44
11. R.H. Kane, Effects of Silicon Content and Oxidation Potential on the Carburization of Centrifugally Cast HK-40, *Corrosion*, Vol 37 (No. 4), 1981, p 187-199
12. T. Shinohara, I. Kohchi, K. Shibata, J. Sugitani, and K. Tsuchida, Development of Nondestructive Technique for Measuring Carburization Thickness and of a New Carburization-Resistant Alloy, *Werkst. Korros.*, Vol 37, 1986, p 410-418
13. W. Zhang, Y. Yang, Q. Liu, Y. Zhu, Q. Zhang, and Z. Hu, Effects of Electromagnetic Stirring and Water Cooling on Structure and Segregation in Centrifugally Cast Al-Si Eutectic Alloy, *Mater. Sci. Technol.*, Vol 14 (No. 4), 1998, p 306-311
14. Y. Yang, Q. Liu, Y. Jiao, Z. Hu, G. Jia, G. Zhang, Y. Gao, and J. Zhang, Solidification Structure of 25Cr-20Ni-Fe-C Alloy by Electromagnetic Centrifugally Casting, Proceedings of International Symposium on Electromagnetic Processing of Materials (Nagoya, Japan), *ISIJ Int.*, Oct 1994, p 420-425
15. Y. Yang, Q. Liu, Y. Jiao, Z. Hu, J. Zhang, and Y. Gao, Effect of Fluid Flow on Eutectic Carbide of Steel HK40, Proceedings of the Second Pacific Rim International Conference on Advanced Materials and Processing (Kyongju, Korea), Korea Institute of Metals and Materials, June 1995, p 149-153
16. J. Szekely, C.W. Chang, and R.E. Ryan, The Measurement and Prediction of the Melt Velocities in a Turbulent, Electromagnetically Driven Recirculating Low Melting Alloy System, *Metall. Trans. B*, Vol 8, 1977, p 333-340
17. H. Fredriksson and A. Olsson, Mechanism of Transition from Columnar to Equiaxed Zone in Ingots, *Mater. Sci. Technol.*, Vol 2 (No. 5), 1986, p 508-516
18. G.S. Cole and G.F. Bolling, Enforced Fluid Motion and the Control of Grain Structures in Metal Castings, *Trans. AIME*, Vol 239 (No. 11), 1967, p 1824-1835
19. W.D. Griffiths and D.G. McCartney, The Effect of Electromagnetic Stirring during Solidification on the Structures of Al-Si Alloys, *Mater. Sci. Eng. A*, Vol 216, 1996, p 47-60
20. K. Nishino and N. Kagawa, Structural Diagram of Austenitic 25%Cr-20Ni-Fe-C Type Alloys, *Tetsu-to-Hagane*, Vol 58 (No. 1), 1972, p 107-118
21. W. Zhang, Y. Yang, Q. Liu, Y. Zhu, and Z. Hu, Numerical Simulation of Fluid Flow in Electromagnetic Centrifugal Casting, *Model. Simul. Mater. Sci. Eng.*, (No. 4), 1996, p 421-432